Effect of a Shielding Cylinder on the Rotor Losses in a Rectifier-loaded PM Machine

H. Polinder, M.J. Hoeijmakers
Electrical Power Processing, Electrical Engineering, Delft University of Technology
Mekelweg 4, 2628 CD Delft, The Netherlands
E-mail: H.Polinder@ITS.TUDelft.NL

Abstract - **The objective of the research project is the development of a high-speed, high-efficiency generator system, consisting of a permanent-magnet (PM) generator loaded with a six-pulse controlled rectifier. In this paper, the effect of a shielding cylinder surrounding the rotor of the PM machine on the rotor losses is investigated. A machine model including the losses in copper, iron, magnets and shielding cylinder is derived and validated by means of measurements. A shielding cylinder is generally not necessary to obtain a sufficiently small angle of overlap, nor effective to reduce the reactive power. It introduces extra rotor losses in the cylinder, but it shields the rest of the rotor, thus avoiding losses in the rotor iron and the magnets. At high speeds, a shielding cylinder reduces the rotor losses; at low speeds, segmenting the magnets is better. The distance between the shielding cylinder and the stator should be large enough to obtain acceptable rotor losses.**

Index terms - **permanent-magnet machine, shielding cylinder, losses, eddy-current losses in magnets, controlled rectifier**

I. Introduction

This paper arises from a research project, the aim of which is the development of a high-speed, high-efficiency generator system. It consists of a permanent-magnet (PM) generator with surface-mounted magnets and a six-pulse controlled rectifier, because these components enable high efficiency, high reliability, high power density, and high speed. The generator system can be applied in hybrid vehicles (Fig. 1), aircraft, vessels, and total energy units.

The objective of this paper is to investigate the effect of a shielding cylinder surrounding the rotor on the rotor losses in rectifier-loaded PM machines, as depicted in Fig. 2. It is important to know the rotor losses, because they heat the rotor, which can only be cooled with difficulty, and the magnets demagnetize if they become too hot. For example, there are NdFeB magnets which demagnetize at about 120° C. A shielding cylinder introduces extra rotor losses in the cylinder, but it shields the rest of the rotor, thus avoiding the losses in the rotor iron and the permanent magnets.

To make the model suitable to optimize the machine design, it is analytic and its parameters are calculated from the dimensions and material properties of the machine.

Several papers describe methods to calculate the losses in shielding cylinders or retaining sleeves in PM machines [1], [2], [3], [4]. Ref. [1] compares the losses in a shielding cylinder to the losses in the solid rotor iron, and shows that when solid rotor iron is used, a cylinder is necessary to obtain acceptable rotor losses. Space harmonics of the magnetic field are considered, because the losses they cause in the shielding cylinder may be important.

Eddy-current losses in permanent magnets are often neglected. This is allowed for plastic bonded or ferrite magnets which have a very high resistivity. However, sintered rare-earth magnets have a much lower resistivity, and the eddy-current losses in these magnets may be important [5]. Several papers discuss methods to calculate these eddy-current losses [6], [7], [8], [9]. Often, simplifying methods are used: the permanent magnets are replaced by cylinders of magnet material [7], [8]. This does not give realistic results when the magnets are segmented to reduce the eddy-current losses in the magnets [5], [8], [9]. In this paper, the eddy-current losses in segmented magnets are considered.

The additional value of this work is that it makes it possible to compare machines with and without shielding cylinder.

The paper first describes the machine model derivation in section II. Next, in section III, the models are validated by means of measurements. In section IV, the derived model is used to calculate the effect of some design parameters on the rotor losses. In section V, some conclusions are drawn.

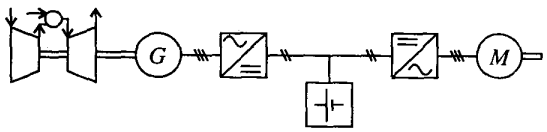

Fig. 1. Drive system of a series-hybrid vehicle consisting of gas turbine, generator, rectifier, accumulator inverter and traction motor.

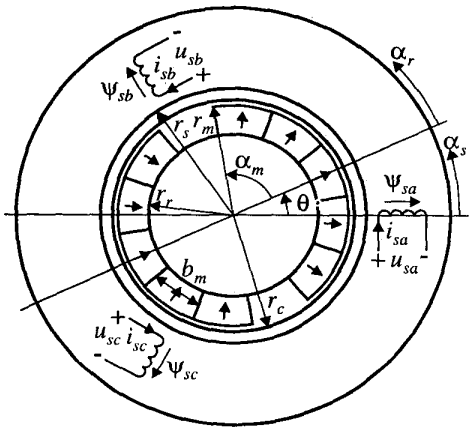

Fig. 2. Two-pole PM machine with shielding cylinder.

II. Model Derivation

This section gives a condensed description of the modelling of the rectifier-loaded PM generator. The derivation of the model is not described thoroughly, because more extensive descriptions of parts of the model has been published in [4], [9], [10], [11], [12]. Instead, the important assumptions, derivation methods and results are given.

A. *Starting-points and Assumptions*

The following starting points are taken in this paper.

- The stator conductors are subdivided into sufficiently small parallel conductors, so that extra losses due to skin effect in the stator conductors are negligible [12].
- A fibre bandage is used as a retainment sleeve to make the rotor strong enough.
- Steady-state operation is considered.
- Ref. [1] and [12] show that a machine with solid rotor iron needs a shielding cylinder to prevent excessive rotor iron losses. Therefore, in the machine without shielding cylinder, laminated rotor iron is assumed.
- There is no star-point connection.

The derivations are based on the following assumptions.

- The magnetic permeability of iron is infinite.
- The relative magnetic permeability of the magnets is one.
- The effect of eddy currents in the stator and the rotor iron and in the magnets on the magnetic field is negligible.
- The shielding cylinder is so thin that it can be replaced by a surface current density in the calculation of the magnetic field and that skin effect is negligible.
- End effects are negligible.

B. *Voltage Equations*

As described in [4], [12], the derivation of the machine model begins with the calculation of the magnetic field in the air gap and the magnets. In this calculation, effects which hardly influence the magnetic field or influence it only locally are neglected. Therefore, the stator and the rotor surface are assumed to be smooth; stator slotting is neglected at this stage.

Under the assumptions mentioned, the magnetic field is a superposition of the fields caused by the permanent magnetization of the magnets, the stator currents, and the current density in the shielding cylinder (if a shielding cylinder is present). The magnetic field is calculated two-dimensionally and in a cylindrical coordinate system, because the effective air gap, which includes the magnets, is large and cylindrical. Space harmonics of the magnetic field are considered, because the losses they cause in the shielding cylinder may be important. The fields are calculated from the differential equation for the magnetic vector potential (Poisson's equation).

The expressions for the magnetic field are used to derive the voltage equations of the PM generator. They form a model of the relation between the terminal voltages and the terminal currents of the machine. These voltage equations are transformed to the stator connected $\alpha\beta$-system using the orthogonal Clarke transformation and the rotor quantities are referred to the stator.

The resulting voltage equations can be written as [4], [12]

$$\begin{cases} \begin{bmatrix} u_{s\alpha} \\ u_{s\beta} \end{bmatrix} = \begin{bmatrix} e_{p\alpha} \\ e_{p\beta} \end{bmatrix} + R_s \begin{bmatrix} i_{s\alpha} \\ i_{s\beta} \end{bmatrix} + L_\sigma \frac{\mathrm{d}}{\mathrm{d}t} \begin{bmatrix} i_{s\alpha} \\ i_{s\beta} \end{bmatrix} + \sum_{k=1,5,7,11,..}^{\infty} L_k \frac{\mathrm{d}}{\mathrm{d}t} \begin{bmatrix} i_{s\alpha}+i_{C\alpha,k} \\ i_{s\beta}+i_{C\beta,k} \end{bmatrix} \\ \begin{bmatrix} 0 \\ 0 \end{bmatrix} = R_{C,k} \begin{bmatrix} i_{C\alpha,k} \\ i_{C\beta,k} \end{bmatrix} + L_k \frac{\mathrm{d}}{\mathrm{d}t} \begin{bmatrix} i_{s\alpha}+i_{C\alpha,k} \\ i_{s\beta}+i_{C\beta,k} \end{bmatrix} \pm kp\Omega L_k \begin{bmatrix} i_{s\beta}+i_{C\beta,k} \\ -i_{s\alpha}-i_{C\alpha,k} \end{bmatrix} \end{cases} \quad (1)$$

where

e_p is the no load voltage,
R_s is the stator resistance,
L_σ is the leakage inductance,
L_k is the main inductance for the kth space harmonic,
$R_{C,k}$ is the cylinder resistance for the kth space harmonic,
$\pm$ is $\begin{cases} + & \text{for } k = 1,7,13,.. \\ - & \text{for } k = 5,11,17.. \end{cases}$
p is the number of pole pairs,
Ω is the mechanical angular speed:

$$\Omega = \frac{\mathrm{d}\theta}{\mathrm{d}t} \quad (2)$$

θ is the rotor position angle (Fig. 2).

The most important parameters of (1) are related to the dimensions (see also Fig. 2) and the material properties in the following way.

$$\begin{bmatrix} e_{p\alpha} \\ e_{p\beta} \end{bmatrix} = \sqrt{\frac{3}{2}} \sum_{k=1,3,5,..}^{\infty} \hat{e}_{p,k} \begin{bmatrix} -\sin(kp\theta) \\ \cos(kp\theta) \end{bmatrix} \quad (3)$$

$$\hat{e}_{p,k} = \frac{(r_m^{2kp} - r_r^{2kp}) r_s^{kp} r_r}{(r_s^{2kp} - r_r^{2kp}) r_m^{kp}} \frac{\pi}{2} \mu_0 l_s N_{s,k} \hat{M}_{p,k} \Omega \quad (4)$$

$$L_k = \frac{(r_c^{2kp} + r_r^{2kp}) r_s^{2kp}}{(r_c^{2kp} + r_s^{2kp})(r_s^{2kp} - r_r^{2kp})} \frac{3\mu_0 \pi l_s N_{s,k}^2}{4kp} \quad (5)$$

$$R_{C,k} = \frac{6 r_s^{2kp} r_c^{2kp}}{(r_c^{2kp} + r_s^{2kp})^2} \frac{\pi l_s \rho_c N_{s,k}^2}{4 r_c \delta_c} \quad (6)$$

where

r_r is the outer radius of the rotor iron,
r_m is the outer radius of the magnets,
r_c is the radius of the middle of the shielding cylinder,
r_s is the inner radius of the stator,
l_s is the stack length of the machine,
$N_{s,k}$ is the number of turns of the kth space harmonic of the conductor density [4], [12],
$M_{p,k}$ is the kth space harmonic of the permanent magnetization,
ρ_c is the resistivity of the shielding cylinder,
δ_c is the thickness of the shielding cylinder, which can be

replaced by the skin depth when the skin depth is smaller than the cylinder thickness.

In this model, the shielding cylinder is represented by two short-circuited windings (one in the α and one in the β-axis) for each space harmonic. For a PM machine without shielding cylinder, the same model can be used when the equations and representing the shielding cylinder are omitted.

C. *Steady-state Voltage Equations and Equivalent Circuits*

In the rest of this paper, two situations are considered, namely steady-state operation with rectifier load, and locked-rotor tests. For these situations, the voltage equations are worked out.

During steady-state operation with rectifier, the relations between the rotor position angle θ, the angular speed of the rotor Ω and the angular frequency of the fundamental time harmonic ω_1 can be written as

$$\Omega = \frac{\omega_1}{p} \quad ; \quad \theta = \frac{\omega_1}{p} t - \frac{\pi}{2p} \tag{7}$$

This is used in the expression for the no-load voltage (3). Furthermore, the time harmonics of which the harmonic number is an integer multiple of three are omitted, because they are not present in the line voltages. Using a complex representation, this expression for the no-load voltage can be written as

$$\begin{bmatrix} e_{p\alpha} \\ e_{p\beta} \end{bmatrix} = \sqrt{\frac{3}{2}} \sum_{n=-\infty}^{\infty} \mathrm{Re}\left\{ \underline{\hat{e}}_{p,6n+1} \mathrm{e}^{\mathrm{j}(6n+1)\omega_1 t} \begin{bmatrix} 1 \\ -\mathrm{j} \end{bmatrix} \right\} \tag{8}$$

Furthermore, the stator currents form a balanced set of three-phase currents without even time harmonics and without time harmonics of which the harmonic number is an integer multiple of three. Using a complex representation, this set of currents can be written in the αβ-system as

$$\begin{bmatrix} i_{s\alpha} \\ i_{s\beta} \end{bmatrix} = \sqrt{\frac{3}{2}} \sum_{n=-\infty}^{\infty} \mathrm{Re}\left\{ \underline{\hat{i}}_{s,6n+1} \mathrm{e}^{\mathrm{j}(6n+1)\omega_1 t} \begin{bmatrix} 1 \\ -\mathrm{j} \end{bmatrix} \right\} \tag{9}$$

By substituting this set of currents in the shielding cylinder voltage equation (the second expression of (1)), the shielding cylinder currents are solved. Substituting the result in the stator voltage equation (the first expression of (1)) results in

$$\begin{bmatrix} u_{s\alpha} \\ u_{s\beta} \end{bmatrix} = \sqrt{\frac{3}{2}} \sum_{n=-\infty}^{\infty} \mathrm{Re}\left\{ \underline{\hat{u}}_{s,6n+1} \mathrm{e}^{\mathrm{j}(6n+1)\omega_1 t} \begin{bmatrix} 1 \\ -\mathrm{j} \end{bmatrix} \right\} \tag{10}$$

where

$$\underline{\hat{u}}_{s,6n+1} = \underline{\hat{e}}_{p,6n+1} + \underline{Z}_{6n+1} \underline{\hat{i}}_{s,6n+1} \quad ;$$

$$\underline{Z}_{6n+1} = R_s + \mathrm{j}(6n+1)\omega_1 L_\sigma + \sum_{k=1,5,7,11,..}^{\infty} \frac{\mathrm{j}(6n+1)\omega_1 L_k R_{C,k}}{R_{C,k} + \mathrm{j} s_{k,6n+1}(6n+1)\omega_1 L_k} \tag{11}$$

where the slip $s_{k,6n+1}$ resulting from the combination of the kth space harmonic and the $|6n+1|$ th time harmonic is given by

$$s_{k,6n+1} = \begin{cases} 1 - \dfrac{kp\Omega}{(6n+1)\omega_1} & \text{for } k = 1,7,13,.. \\ 1 + \dfrac{kp\Omega}{(6n+1)\omega_1} & \text{for } k = 5,11,17,.. \end{cases} \tag{12}$$

The equivalent circuit for the $|m|$th ($m = 6n+1$) time harmonic is depicted in Fig. 3. For the locked-rotor tests, the same equivalent circuit can be used when it is taken that the no-load voltages are zero and the slip is one for all harmonics.

Although the derived voltage equations are suitable for the calculation of the terminal voltages and the terminal currents, they only consider a part of the losses in the machine, namely the copper losses. They neglect other important losses, such as

- the eddy-current loss in the magnets,
- the iron losses, and
- the losses due to the stator slotting.

Therefore, these losses are modelled and incorporated in the machine model in the next subsections.

D. *Eddy-current Losses in Magnets*

Ref. [6] shows that it is possible to determine the eddy-current losses in permanent magnets in a very accurate way, considering flux redistribution due to the eddy currents. However, here a simpler model is used [9], [12], which gives a useful approximation of the eddy-current losses in segmented permanent magnets. In [12], it is shown that the eddy-current losses in the magnets due to the higher space harmonics are small compared to the losses caused by the fundamental space harmonic. Therefore, the higher space harmonics of the magnetic field are not considered here.

The eddy-current losses in the magnets are determined using the cross-section of the magnet of Fig. 4. The eddy-current losses are calculated in the same way as the eddy current losses in laminated iron [13]. Therefore, the following assumptions are used.

- The magnetic flux density B only has a (radial) y-component, which is a reasonable assumption for the fundamental space harmonic.

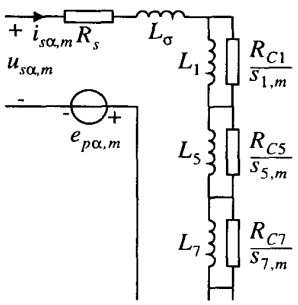

Fig. 3. Equivalent circuit of the PM machine for the $|m|$th time harmonic. The fundamental, the fifth and the seventh space harmonic are depicted, for the other space harmonics, the circuit can be extended in the same way.

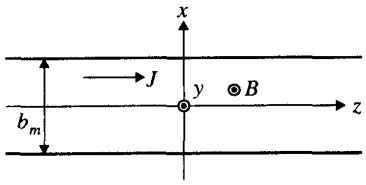

Fig. 4: Cross-section of a magnet in a rectangular coordinate system.. The current density J flows in the (axial) z-direction, the magnetic flux density is in the (radial) y-direction perpendicular to the plane of the drawing. The x-direction is the tangential direction.

- As earlier mentioned, the effect of eddy currents in the magnets on the magnetic field is negligible.
- End effects are negligible, so that the current density only has a component in the (axial) z-direction. This assumption is reasonable if the magnet length in the z-direction is much larger than the magnet width b_m, otherwise, the losses are overrated.
- The magnet width b_m is so small that the magnetic flux density can be considered constant over the magnet width.

With this, the eddy-current losses in the magnets per unit volume are calculated as

$$k_m = \frac{b_m^2}{12\rho_m}\left(\frac{dB}{dt}\right)^2 \tag{13}$$

where ρ_m is the resistivity of the magnets.

Comparable expressions are derived in, for example, [13] for the eddy-current losses in laminated iron.

Because of the assumptions used, the losses are not calculated very accurately. However, it is expected that for machines with segmented magnets, the results are much better than the results calculated assuming a cylinder of magnet material.

The eddy-current losses in the magnets are represented by a magnet loss resistance in the equivalent circuit [9], [12], as depicted in Fig. 5. The magnet loss resistance is given by

$$R_M = \frac{6r_s^{2p}r_m^{2p}}{(r_s^{2p}+r_m^{2p})^2}\frac{3\rho_m\pi^2 r_m l_s N_{s,1}^2}{l_m b_m^2 p^3 \alpha_m} \tag{14}$$

where

l_m is the magnet length in the direction of magnetization, and

α_m is half the magnet pole arc (see Fig. 2), which is subdivided in magnets of width b_m.

The first term in this expression originates from referring the rotor quantities to the stator; the same term is present in the expression for the shielding cylinder resistance (6).

E. Iron Losses

The classical theory about iron losses separates between hysteresis losses $P_{Fe,h}$ and eddy-current losses $P_{Fe,cl}$ [13]:

$$P_{Fe,h} \propto \omega \hat{B}^S \tag{15}$$

$$P_{Fe,cl} \propto \begin{cases} \omega^2\hat{B}^2 & \text{at low frequencies} \\ \omega^{1.5}\hat{B}^2 & \text{at high frequencies} \end{cases} \tag{16}$$

where ω is the angular frequency, and S is the Steinmetz constant, which is approximately 2.

In modern literature, often a third term is added: the excess losses [13]:

$$P_{Fe,e} \propto \omega^{1.5}\hat{B}^{1.5} \tag{17}$$

In this study, a simpler model for the iron losses per unit mass is used [10], [12], which is comparable to the model used in [14]:

$$k_{Fe} = c_{Fe}k_{Fe,0}\left(\frac{\omega}{\omega_0}\right)^{1.5}\left(\frac{\hat{B}}{\hat{B}_0}\right)^2 \tag{18}$$

where $k_{Fe,0}$ is the iron losses per unit mass at a given angular frequency ω_0 and magnetic flux density $\hat{B}_0$, and c_{Fe} is a dimensionless empirical correction factor.

The claim that (18) is a useful expression for the iron losses, can be made plausible by comparing it to the equations for the hysteresis, the eddy-current and the excess losses.

- At high frequencies, the iron losses are dominated by the eddy-current losses and the excess losses, which are both proportional to $\omega^{1.5}$.
- At medium frequencies, (18) is an approximation of the sum of the three contributions.
- That (18) is not valid at low frequencies does not matter, because these frequencies do not occur.

The measurements reported in this study [10], [12] and in [14] indicate that (18) is useful for frequencies above 400 Hz.

Further, the calculation of the iron losses is mainly based on the following assumptions.

- The losses due to higher space harmonics are negligible.
- The losses can be calculated as the sum of the losses due to the time harmonics.

The iron losses are represented by iron loss resistances in the equivalent circuit of the machine. Because it is assumed that the iron losses are proportional to $\omega^{1.5}$, the resistances are frequency dependent. In the equivalent circuit of Fig. 5, the stator iron losses are represented by the resistance R_{sFe}, and the rotor iron losses are represented by the resistance R_{RFe}.

It is taken into account that a part of the stator iron losses is caused by the leakage fluxes. Therefore, the iron loss resistance R_{sFe} is not only connected in parallel to the main inductance, but also to a part of the leakage inductance, as shown in Fig. 5.

A stray loss resistance $R_{\sigma Fe}$ is incorporated to represent the stray losses. Stray losses are for example eddy-current losses in the end regions induced by leakage fluxes and iron losses caused by the higher space harmonics of the magnetic field of the stator currents [15]. Because stray losses are basically iron losses, they are assumed to be the same function of the angular frequency as the other iron losses.

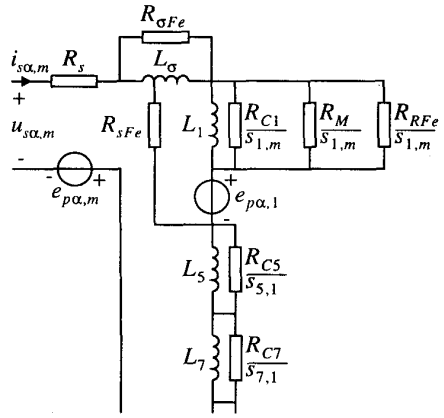

Fig. 5: Equivalent circuit of the PM machine for the $|m|$th time harmonic. For the fundamental time harmonic, $e_{p\alpha,1}$ has a value, $e_{p\alpha,m}=0$; for the higher time harmonics, $e_{p\alpha,m}$ has a value, $e_{p\alpha,1}=0$.

F. *Extra Losses due to Stator Slotting*

In the generator model described above, the stator was assumed to be smooth and cylindrical. However, most machines have stator slots, which may cause considerable losses in the shielding cylinder. The modelling of the field and the eddy currents due to the stator slotting is quite complicated. It is questionable whether analytic methods are suitable to determine these losses.

In [2], the magnetic vector potential in a slotted air gap with a conducting magnet retaining ring is calculated analytically. However, this was not done for a cylindrical model of the machine but for a linear model, and the slots were approximated by triangular extensions of the air gap where the field is one-dimensional.

In this study, the conformal transformation described in [12] and [16] was used to calculate the amplitude of the pulsation of the magnetic flux density at the cylinder radius. Also in [17], a conformal transformation is used to calculate this pulsation.

Next, the current in the shielding cylinder is calculated. In [17] and [18], this is done on the assumption that the effect of the current in the cylinder on the magnetic field is negligible, which is not necessarily the case for larger machines. Therefore, the current density in the shielding cylinder is calculated using the voltage equations of the windings representing the shielding cylinder derived in section II.B. The voltage induced by the pulsation in these short-circuited windings is calculated after which the current in these windings is calculated. Because these windings do not only have a resistance but also an inductance, the effect of the currents on the magnetic field is considered.

It should be noted that the extra losses caused by the stator slotting are not independent of the losses caused by the space harmonics of the magnetic field of the stator currents. Therefore, the current density caused by the stator currents and the current density caused by the stator slotting are added before the losses are calculated.

Because of the assumptions used, the results are not expected to be very accurate, but they satisfy to get an indication and to identify some trends. For a more extensive description of the calculation is referred to [12].

G. *Harmonic Analysis of the Rectifier-loaded Generator*

There are several ways of calculating the voltage and current waveforms of the machine loaded with a six-pulse controlled rectifier as depicted in Fig. 6. It is possible to take (1), model the thyristors and determine the waveforms by means of numerical integration in the time domain. Even when only the first space harmonic is considered, the calculated waveforms will be quite accurate. Losses due to higher space harmonics, iron losses and eddy-current losses in the magnets can then be calculated when the current waveforms are known.

However, in this study, the model of the PM generator is combined with a model of the controlled rectifier and the resulting equations are solved in the frequency domain, which has two important advantages:

- the steady-state performance can be determined without considering the transient interval, and
- a machine model with frequency-dependant parameters as derived in this study can be used.

Because the way the waveforms are calculated is not of primary importance and has been published before [11], [12], [19], it is not reported here.

III. Model Validation

For the validation of the derived models, two types of experiments have been used, namely locked-rotor tests and measurements of voltage and current waveforms of the rectifier-loaded PM machine.

A. *Locked-rotor Tests*

Locked-rotor tests are used to validate the models for the losses. During these tests, the rotor is locked, and a sinusoidal voltage of variable frequency is supplied to two of the machine terminals. From the measured voltage, current and power, the measured resistance and inductance are derived.

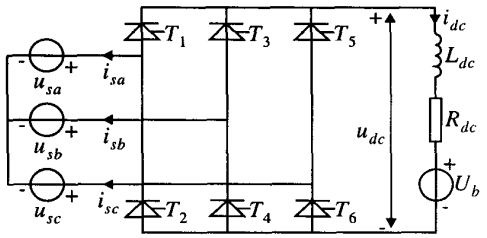

Fig. 6. Generator feeding a DC voltage source via a controlled rectifier.

The measured values of the resistance and inductance are compared to calculated values. These calculated values are obtained from the equivalent circuit of Fig. 5, which is valid for the machine during the locked-rotor tests when it is substituted that the no-load voltage is zero and that the slip is one for all harmonics.

With the locked-rotor tests, the resistance and the inductance for sinusoidal voltages and currents are measured. These sinusoidal voltages and currents are comparable to the harmonics during rectifier load. Therefore, these locked-rotor tests are valuable for the validation of the machine model.

Fig. 7 depicts the results of the locked-rotor tests of a machine with shielding cylinder. The measured and calculated results correlate reasonably. For the higher space harmonics, the model is neither verified nor refuted, because the effect of the space harmonics is small compared to other losses.

At low frequencies, only the losses in the stator coils are measured, other losses are negligible. At frequencies between 10 and 100 Hz, also the losses in the shielding cylinder are measured. Above about 300 Hz, the shielding cylinder completely shields the rotor, and the losses in the shielding cylinder hardly increase. At frequencies above 1 kHz, iron losses cause a further increase of the measured resistance.

Fig. 8 gives the results of the locked-rotor tests of a PM machine without shielding cylinder.

Again, at low frequencies, only the losses in the stator coils are measured. At frequencies above 500 Hz, iron losses and eddy-current losses in the magnets cause an increase in the measured resistance. In contrast to what was assumed earlier, the effect of the eddy currents in the magnets on the magnetic field in the air gap is not negligible at frequencies above 10 kHz. This is modelled by connecting the magnet loss resistance in parallel to the inductance L_1 (see Fig. 5), where it effects the magnetic field in the air gap. From the reasonable correlation between measurements and calculations, it is concluded that the model is useful.

B. Voltage and Current Waveforms with Rectifier Load

To validate the complete model, also voltage and current waveforms of the rectifier-loaded machine are measured and calculated. Fig. 6 depicts the experimental setup. The same PM machine is used for the locked-rotor tests depicted in Fig. 8.

Fig. 9 depicts measured and calculated line voltage and phase current waveforms of a PM machine without shielding cylinder. There is no inductance between the rectifier and the voltage source in the DC-circuit. Therefore, the current in the DC-circuit i_{dc} is not constant and when a phase is conducting, the terminal line voltage is equal to the voltage of the voltage source U_b. Again, the correlation is good.

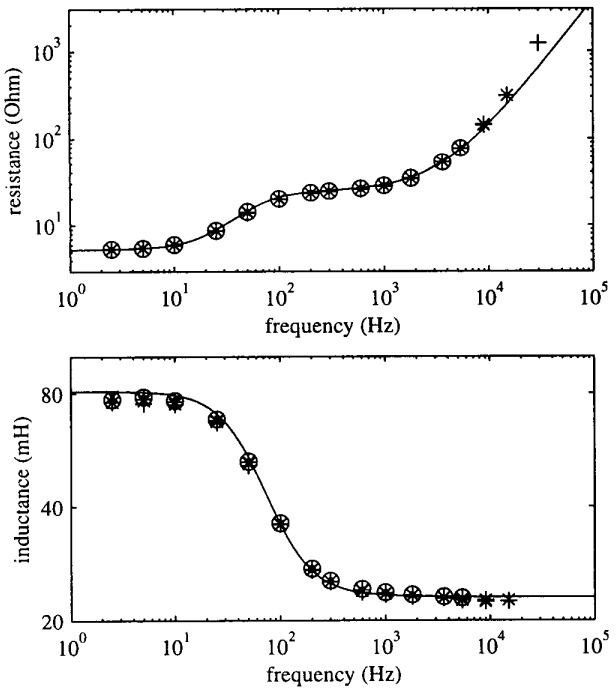

Fig. 7. Measured (+,×, *,○,· at currents from 0.1 A up to 2 A) and calculated (–) resistance and inductance during the locked-rotor tests of a machine with shielding cylinder.

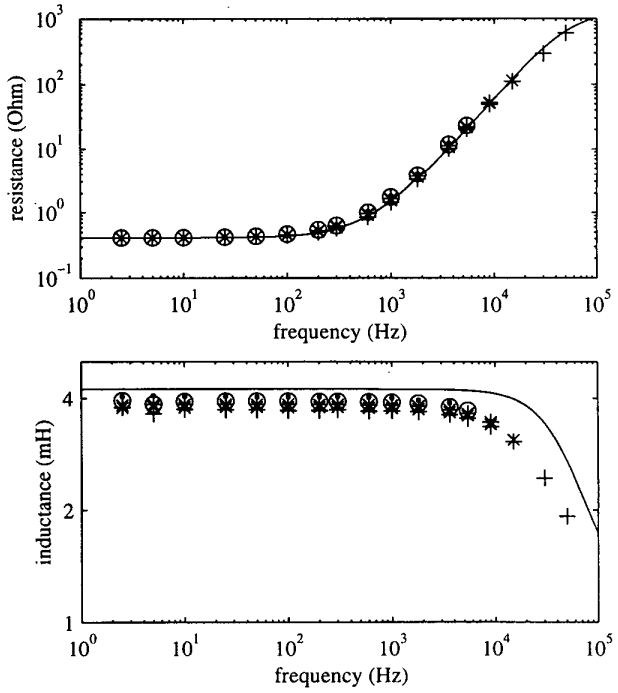

Fig. 8. Measured (+,×, *,○,· at currents from 0.2 A up to 5 A) and calculated (–) resistance and inductance during the locked-rotor tests of a PM machine without shielding cylinder.

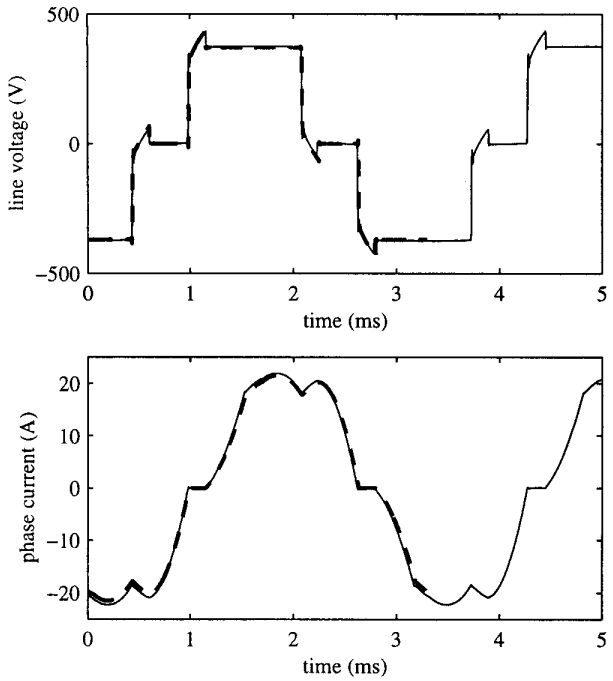

Fig. 9. Measured (–) and calculated (- -) voltage and current waveforms of a rectifier-loaded permanent- magnet machine without shielding cylinder.

IV. Generator Design

To illustrate the usefulness of the derived model, it is used to investigate some important design aspects of PM generators, such as the effects of the shielding cylinder, the magnet width, the rotational speed and the shielding cylinder radius.

Fig. 10 depicts the calculated voltage and current waveforms of the same rectifier-loaded PM machine with and without shielding cylinder. The voltage of the voltage source in the DC circuit and the power delivered to this source are the same.

The effect of the addition of a shielding cylinder is that the angle of overlap decreases, as could be expected because the commutation inductance decreases. However, the shielding cylinder is not necessary to obtain a sufficiently small angle of overlap, as is the case in a rectifier-loaded electrically-excited synchronous machine, which usually needs a damper to make commutation possible. This is caused by the larger air gap in a PM machine, which results in a smaller inductance.

The fact that the shielding cylinder reduces the angle of overlap does not mean (as is sometimes suggested) that the machine with a shielding cylinder supplies less reactive power. The phase angles between the fundamental time harmonics of the phase currents, the terminal voltages and the no-load voltages hardly depends on the presence of a shielding cylinder.

Fig. 11 depicts the rotor losses of a machine with and without shielding cylinder based on the derived model. From this figure, important conclusions can be drawn.

1) The rotor losses in a machine without shielding cylinder are approximately proportional to the square of the magnet width and the square of the frequency, as earlier shown in [9]. In this case, the most important part of the rotor losses is the eddy-current losses in the magnets.

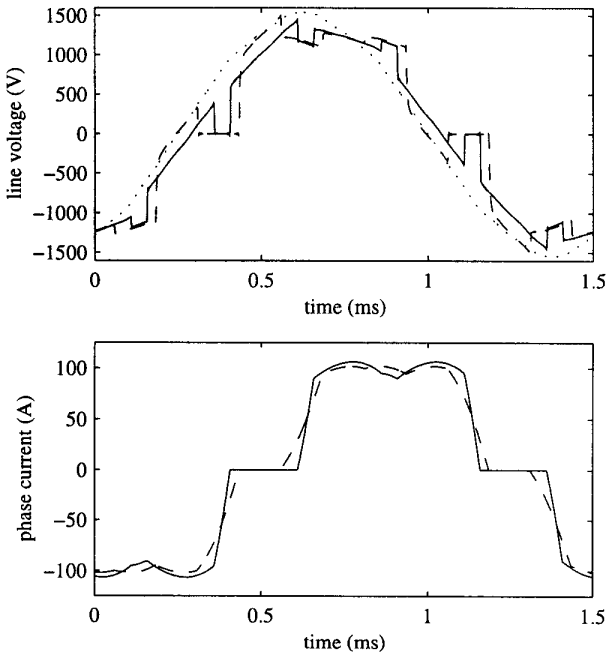

Fig. 10. Calculated line voltage and phase current waveforms of the same rectifier-loaded PM machine without (- -) and with (–) shielding cylinder. The no-load line voltage is depicted dotted (..).

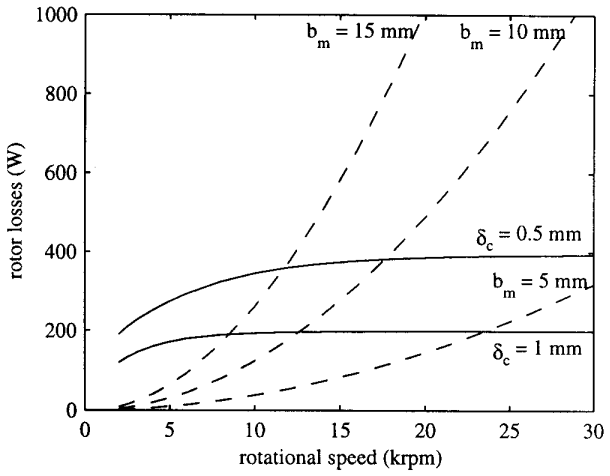

Fig. 11. Calculated rotor losses as a function of the generator speed, with cylinder for different values of the cylinder thickness δ_c (–), and without cylinder for different values of the magnet width b_m (- -). Output power and voltage are proportional to speed; at 20 krpm, the output power is 120 kW.

2) In a machine with shielding cylinder, the rotor losses hardly depend on the frequency, and they are inversely proportional to the shielding cylinder thickness. This is of course only valid as long as skin effect in the cylinder is negligible; when skin effect is not negligible, the rotor losses increase with square root of the frequency.
3) A general statement about the usefulness of a shielding cylinder is not possible. At high speeds, a shielding cylinder is an effective way to reduce the rotor losses; at low speeds, segmenting the magnets may be better.

Fig. 12 depicts the rotor losses as a function of the shielding cylinder radius. From this figure, it is concluded that the distance between the stator surface and the cylinder is very important. If the distance between the stator surface and the cylinder is large, only the fundamental space harmonic causes losses in the shielding cylinder. If the distance between the stator surface and the cylinder is too small, the losses due to the higher space harmonics and stator slotting become excessive.

V. Conclusions

An analytic model suitable to investigate the effect of a shielding cylinder on the rotor losses in a PM machine loaded with a six-pulse controlled rectifier is given. The model includes the most important electromagnetic losses, such as the copper losses in the shielding cylinder and the stator, the iron losses, and the eddy-current losses in the magnets. The model is validated by means of measurements.

In a machine with solid rotor iron, a shielding cylinder is necessary to obtain acceptable rotor losses. In a machine with laminated rotor iron, a shielding cylinder is usually not necessary to obtain a sufficiently small angle of overlap, nor effective to reduce the reactive power. A general statement about the usefulness of a shielding cylinder is not possible: at high speeds, a shielding cylinder is an effective way to reduce the rotor losses; at low speeds, segmenting the magnets is better. The distance between the shielding cylinder and the stator should be large enough to obtain acceptable rotor losses.

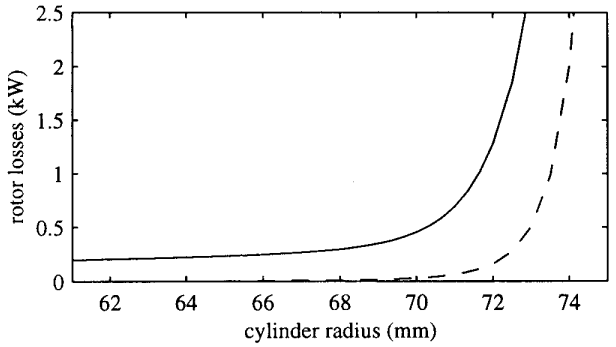

Fig. 12. Calculated rotor losses as a function of the cylinder radius r_c at a speed of 20 krpm and a cylinder thickness of 0.5 mm, at an output power of 120 kW (–) and in no-load (- -).

References

[1] J.L.F. van der Veen, L.J.J. Offringa, A.J.A. Vandenput, "Minimizing rotor losses in high-speed high-power permanent magnet synchronous generators with rectifier load," *IEE Proceedings - Electric Power Applications*, vol 144, pp. 331-337, 1997.

[2] N. Boules, "Impact of slot harmonics on losses of high-speed permanent magnet machines with a magnet retaining ring," *Electric Machines and Electromechanics*, vol. 6, pp. 527-539, 1981.

[3] S.M. Abu Sharkh, M.R. Harris, N. Taghizadeh Irenji, "Calculation of rotor eddy-current loss in high-speed PM alternators," in *Proceedings of the Eighth International Conference on Electrical Machines and Drives*, Cambridge, 1997, pp. 170-174.

[4] H. Polinder, M.J. Hoeijmakers, "Modelling a PM machine with shielding cylinder," in *Proceedings of the Ninth International Conference on Electrical Machines and Drives*, Canterbury, 1999, pp. 16-20.

[5] G. Henneberger, W. Schleuter, "Servoantriebe für Werkzeugmaschinen und Industrieroboter, Teil 2: Bürstenlose Gleichstrommotoren und Zukunftsaussichten," *Elektrotechnische Zeitschrift*, vol. 110, pp. 274-279, 1989.

[6] F. Deng, "Commutation-caused eddy-current losses in permanent magnet brushless DC motors," *IEEE Transactions on Magnetics*, vol. 33, pp. 4310-4318, 1997.

[7] N. Boules, W.-R. Canders, H. Weh: "Analytische Bestimmung des Nutungseinflusses auf die Feldverteilung und die Wirbelstromverluste in dauermagneterregten Synchronmaschinen," *Archiv für Elektrotechnik*, vol. 62, pp. 283-293, 1980.

[8] N. Schofield, K. Ng, Z.Q. Zhu, D. Howe: "Parasitic rotor losses in a brushless permanent magnet traction machine," in *Proceedings of the Eighth International Conference on Electrical Machines and Drives*, Cambridge, 1997, pp. 200-204.

[9] H. Polinder, M.J. Hoeijmakers, "Eddy-current losses in the segmented surface-mounted magnets of a PM machine," *IEE Proceedings - Electric Power Applications*, vol. 146, pp. 261-266, 1999.

[10] H. Polinder, M.J. Hoeijmakers, "Modelling iron losses in high speed PM machines", in *Proceedings of the Eighth International Conference on Electrical Machines*, Helsinki, 2000, in press.

[11] H. Polinder, M.J. Hoeijmakers, L.J.J. Offringa, W. Deleroi, "Harmonic analysis of a PM machine with rectifier," in *Proceedings of the Sixth International Conference on Electrical Machines*, Vigo, 1996, vol. 2, pp. 63-68.

[12] H. Polinder, *On the losses in a high-speed permanent-magnet generator with rectifier - with special attention to the effect of a damper cylinder.* PhD Dissertation, Delft University of Technology, 1998 (Delft: EburonP&L, 1998).

[13] G. Bertotti, *Hysteresis in Magnetism for physicists, materials scientists and engineers*. San Diego: Academic Press, 1998.

[14] F.G.G. de Buck, P. Gistelink, D. de Backer, "A simple but reliable loss model for inverter-supplied induction motors," *IEEE Transactions on Industry Applications*, vol. 20, pp. 190-202, 1984.

[15] C.N. Glew, "Stray load losses in induction motors: a challenge to academia," *Power Engineering Journal*, vol. 12, pp. 27-32, 1998.

[16] Z.Q. Zhu, D. Howe, E. Bolte, B. Ackermann, "Instantaneous Magnetic Field distribution in brushless permanent-magnet dc motors, part I - IV," *IEEE Transactions on Magnetics*, vol. 29, pp. 124-158, 1993.

[17] I. Takahashi, T. Koganezuwa, G. Su, K. Ohyama, "A super high speed PM motor drive system by a quasi-current source inverter," *IEEE Transactions on Industry Applications*, vol. 30, pp. 683-690, 1994

[18] J.R. Hendershot, T.J.E. Miller, *Design of brushless permanent-magnet motors*. Hillsboro: Magna Physics Publishing, 1994.

[19] S. Bolognani, G.B. Indri, "A study of converter-fed synchronous machines by means of Fourier analysis," *IEEE Transactions on Industry Applications*, vol. 16, pp. 203-210, 1980.